

Supplemental Figures

Figure S1

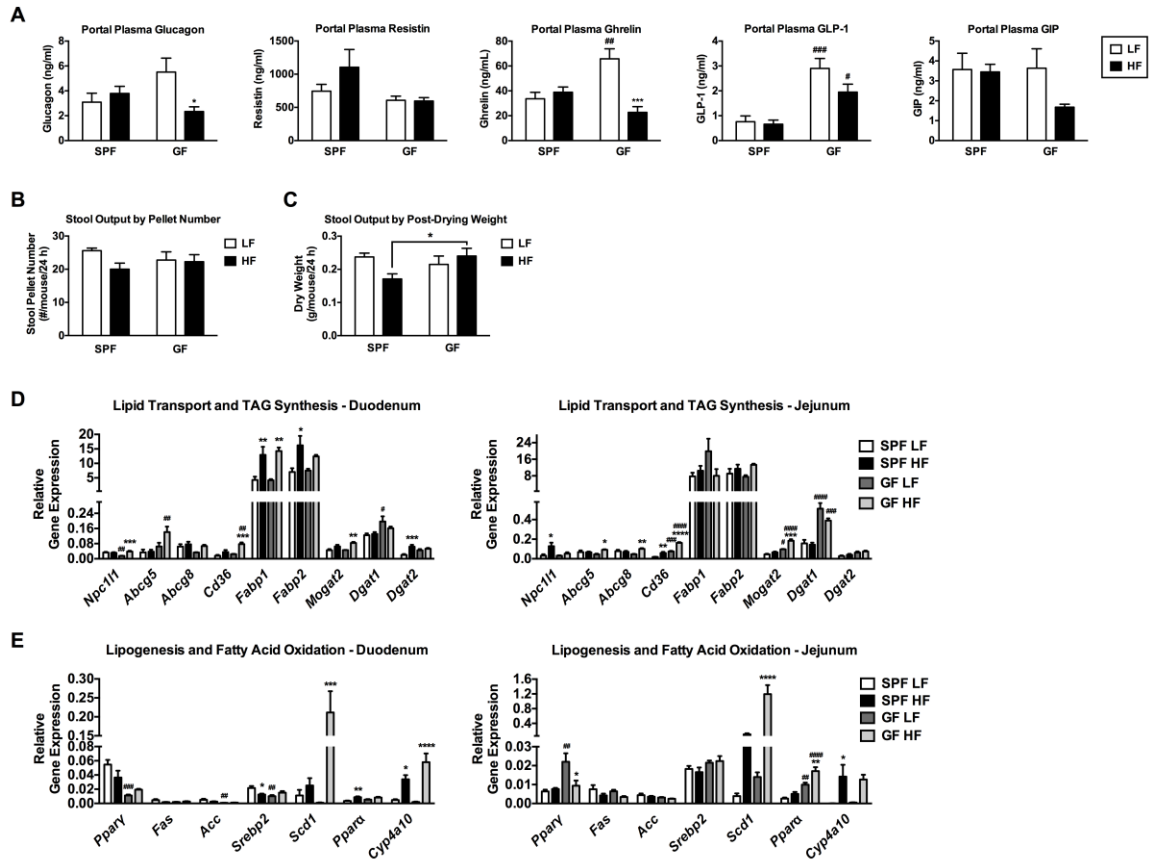


Figure S2

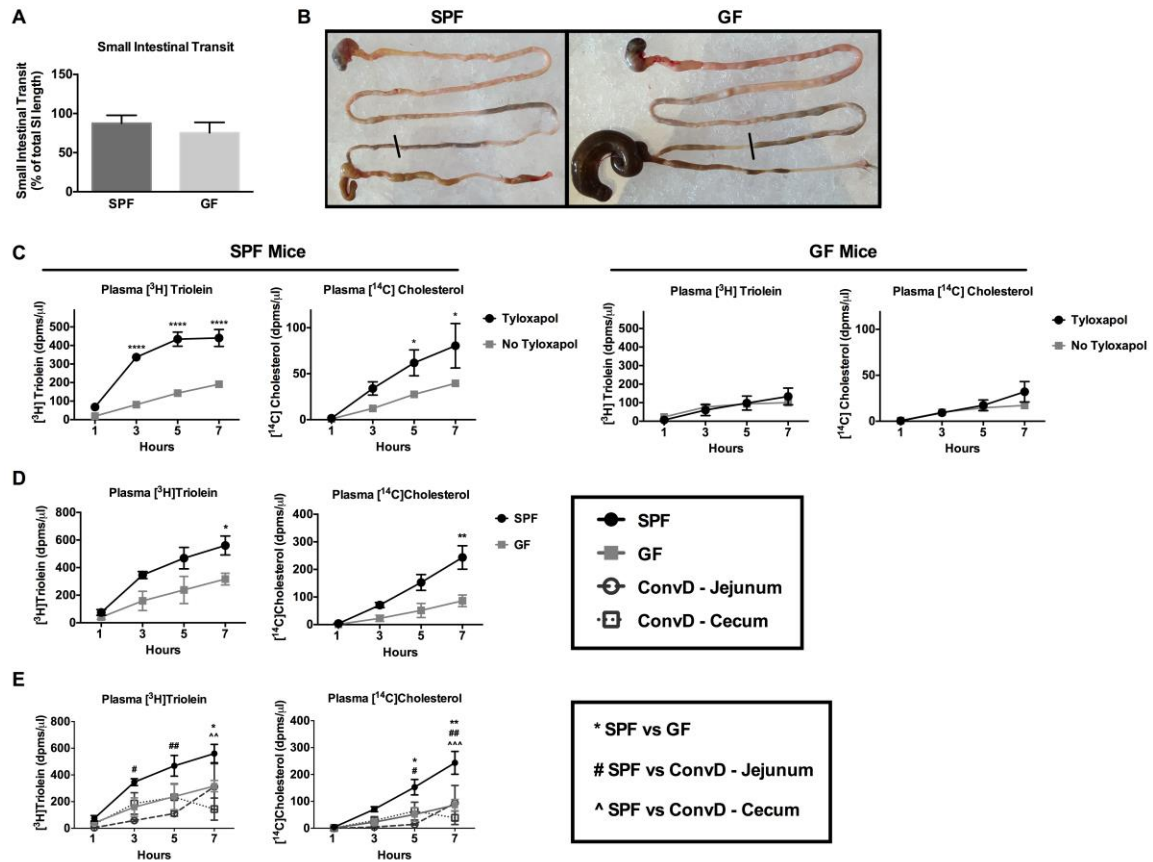


Figure S3

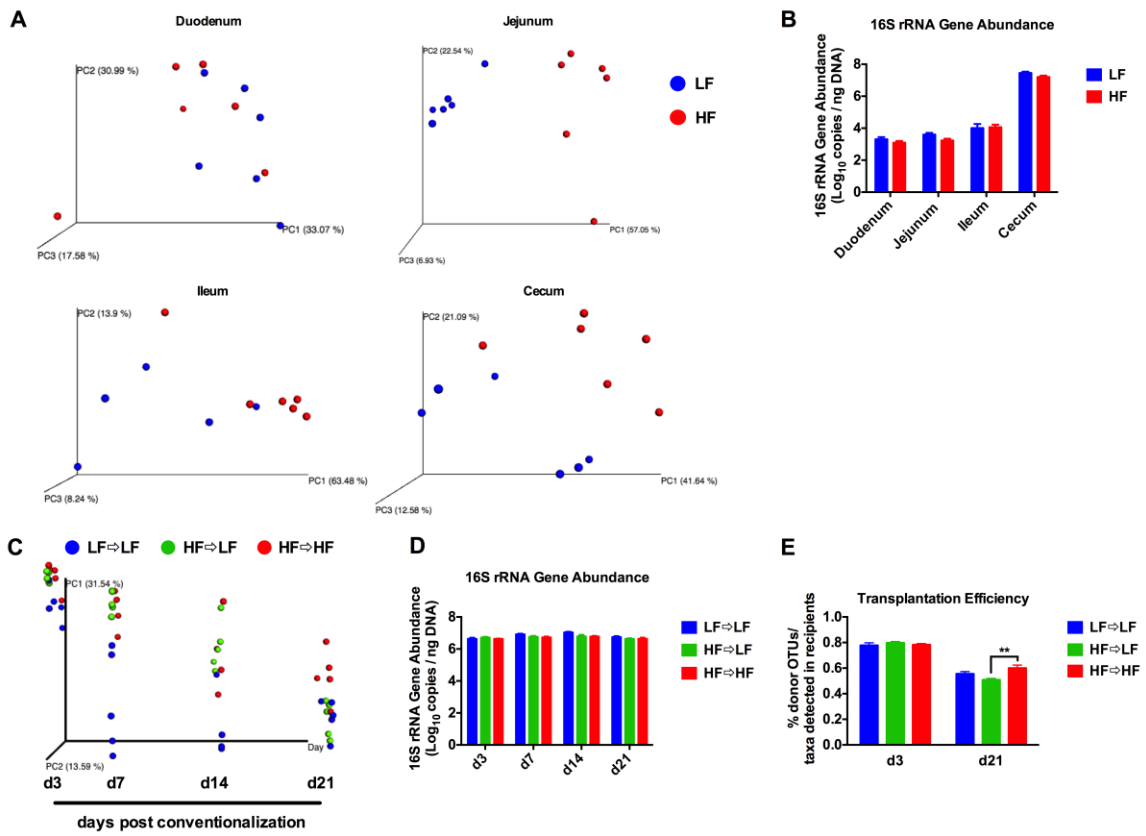


Figure S4

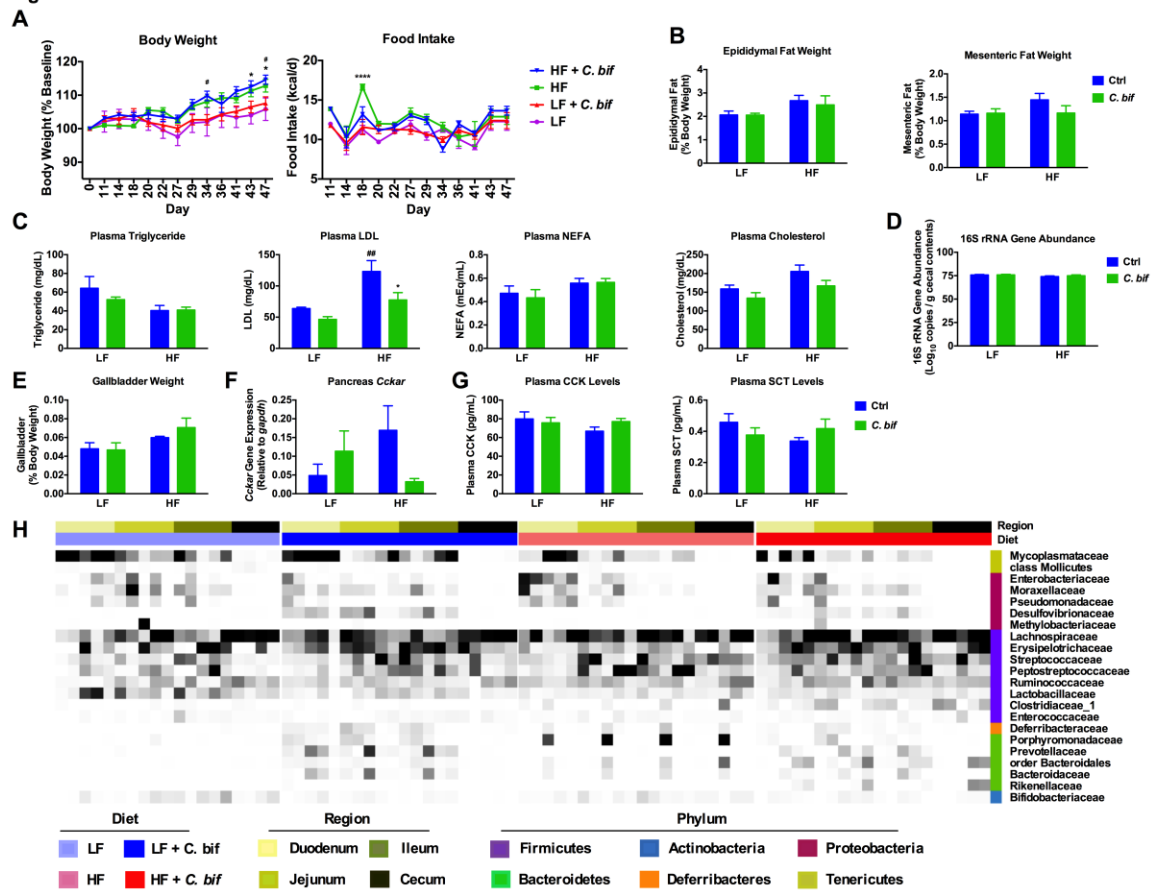


Figure S5

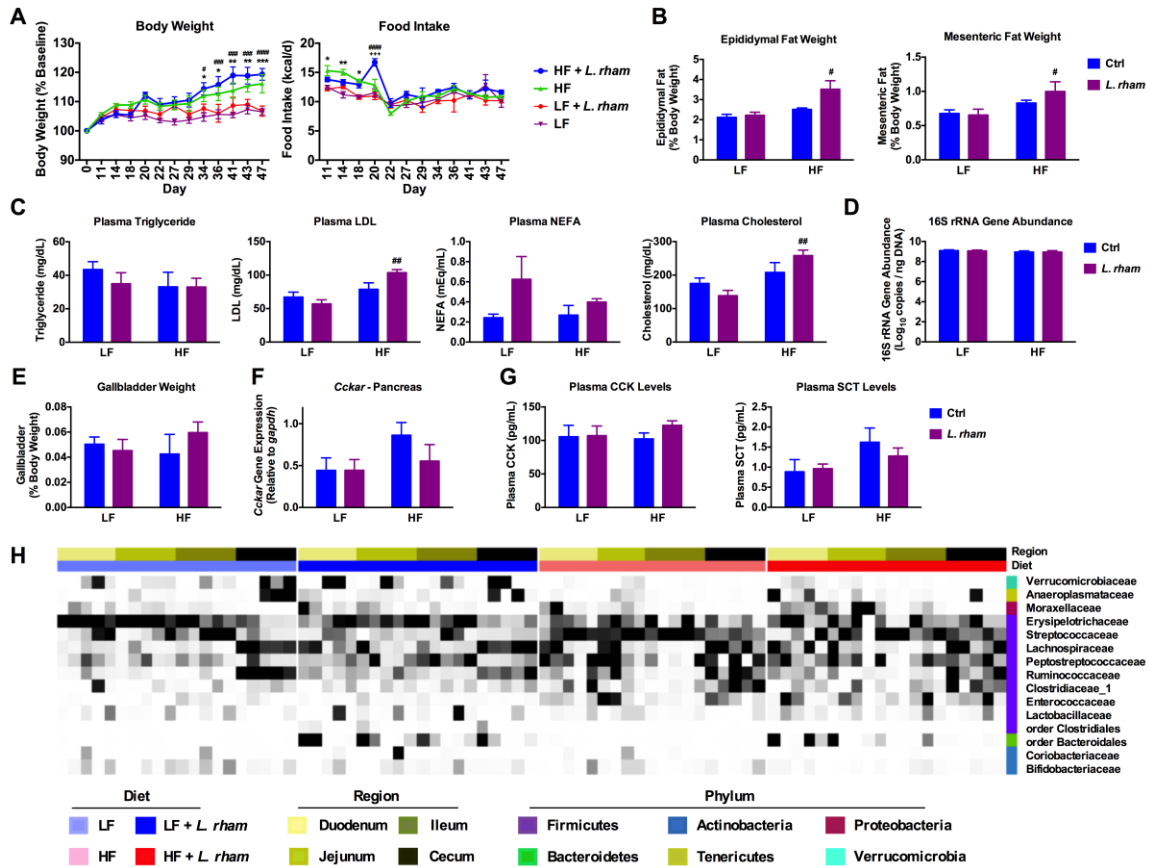
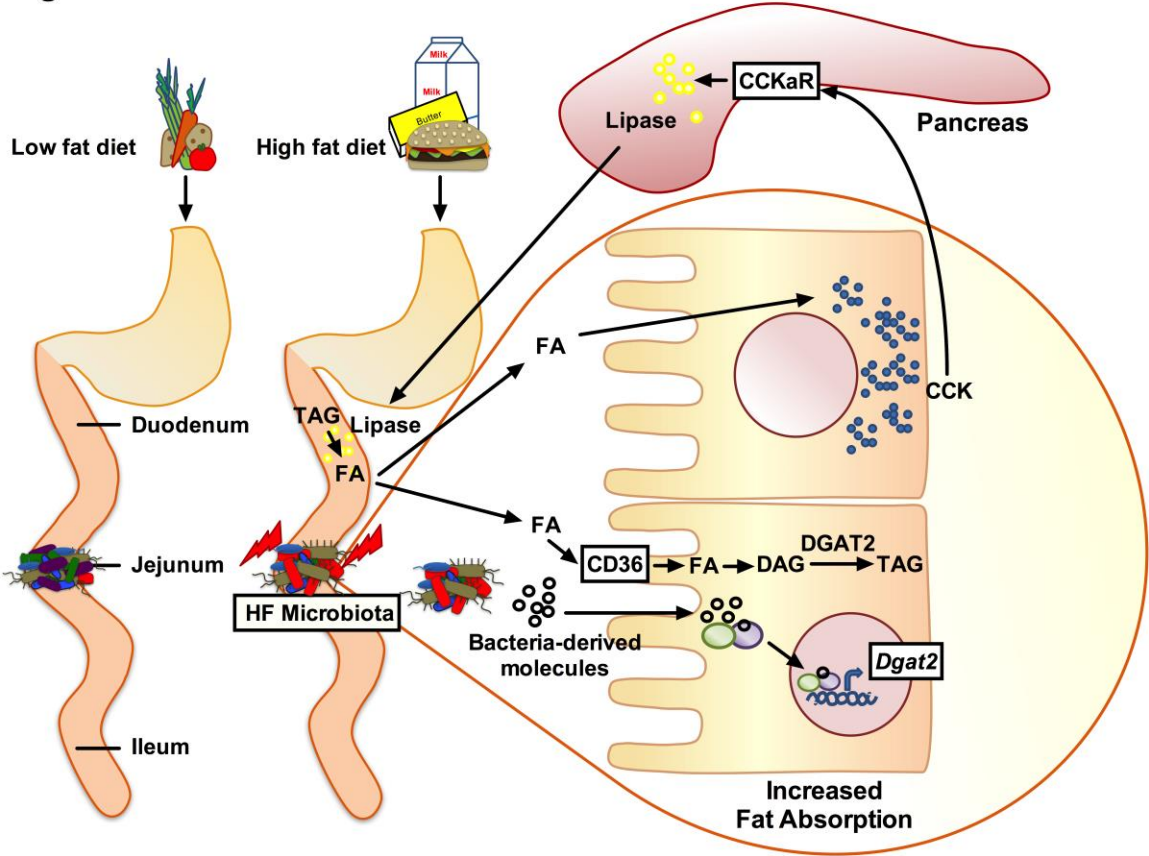


Figure S6



Supplemental Figure Legends

Figure S1 (related to Figure 1). Gut peptide hormone and gene expression analyses in SPF vs GF mice. SPF and GF mice were fed a low fat (LF) or high fat (HF) diet for 4 weeks. **A)** Glucagon, resistin, ghrelin, gastric inhibitory polypeptide (GIP), and glucagon like peptide-1 (GLP-1) were measured in portal plasma. **B-C)** Bedding was changed and collected 24 hours later and stool pellets were counted to determine pellet number per mouse per 24 hours. Stool pellets were dried overnight and weighed to measure grams of dry weight per mouse per 24 hours. **D-E)** mRNA levels of genes related to fat transport and TAG synthesis (**C)** including Niemann-Pick C1-Like1 (*Npc1L1*), ATP- binding cassette transporter subfamilies G5 and G8 (*Abcg5*, *Abcg8*), cluster of differentiation 36/fatty acid translocase (*Cd36*), fatty acid binding proteins (*Fabp1*, *Fabp2*), monoacylglycerol O-acyltransferase 2 (*Mogat2*), diacylglycerol O-acyltransferase 2 (*Dgat2*) or lipogenesis and fatty acid oxidation (**D)** including peroxisome proliferator-activated receptor gamma (*Ppar γ*), fatty acid synthase (*Fas*), acetyl coA carboxylase 1 (*Acc*), sterol regulatory element-binding protein 2 (*Srebp2*), stearoyl-coA desaturase-1 (*Scd1*), peroxisome proliferator-activated receptor alpha (*Ppar α*) and cytochrome p450 family 4 subfamily a polypeptide 10 (*Cyp4a10*) were measured in the duodenum and jejunum via qRT-PCR. Data are shown as means +/- SEM (n=5-6 A; n=6-9 B-C; n=5-6 D-E). * $p \leq 0.05$ (LF vs HF), # $p \leq 0.05$ (SPF vs GF).

Figure S2 (related to Figure 2). Small intestinal transit in SPF vs GF mice. SPF and GF mice were gavaged with 0.5% activated charcoal and 1% methylcellulose delivered in corn oil for 2 hours to determine distance traveled. **A)** Intestines were collected and the distance of charcoal traveled was expressed as a percentage of total small intestine

length. **B)** Pictures of intestine were taken to display distance of charcoal traveled. **C)** SPF and GF mice were treated for 10 minutes with or without tyloxapol followed by gavage with [³H]triolein and [¹⁴C]cholesterol and plasma collected over seven hours. **D)** SPF and GF mice raised in pine shavings and treated with tyloxapol for 10 minutes followed by gavage with [³H]triolein and [¹⁴C]cholesterol and plasma collected over seven hours. **E)** GF mice were conventionalized with standard chow-derived jejunal or cecal microbiota, maintained on donor chow diet, and radiolabeled lipid absorption was measured as shown in **(D)**. Data were pooled across 1-3 independent experiments and are shown as means +/- SEM (n= 3 A-B; n=5-11 C, n = 3-6 D, n = 2-6 E). * p ≤ 0.05.

Figure S3 (related to Figure 4 and Tables 1-2). Characterization of LF and HF microbiota. A-B) SPF and GF mice were fed a low fat (LF) or high fat (HF) diet for 4 weeks. **A)** 16S rRNA amplicon sequencing was performed in the small intestine and cecum. PCoA plots of Bray Curtis dissimilarity indices are shown for each region. **B)** Total 16S copy number was measured via qRT-PCR and expressed as per ng DNA. **C-E)** Germ free (GF) mice were conventionalized with jejunal microbiota collected from mice shown in A-B. 16S rRNA amplicon sequencing was performed in the stool. PCoA plots of Bray Curtis dissimilarity indices are shown for each time point following conventionalization (day 3, 7, 14, 21) with LF jejunal microbes in mice fed a LF diet (LF⇒LF; blue), HF jejunal microbes in mice fed LF diet (HF⇒LF; green), or HF jejunal microbes in mice fed a HF diet (HF⇒HF; red). **D)** Total 16S copy number was measured in stool via qRT-PCR and expressed as per ng DNA. **E)** Transplantation efficiency was calculated by determining the percentage of oligotypes shared between the donor jejunal microbiota and the recipients in stool at days 3 and 21 following conventionalization. Data are shown as means +/- SEM (n=6 A-B; n=5 C-E).

Figure S4 (related to Figure 5). Supplementation of *Clostridium bifermentans* under LF and HF conditions. SPF mice were treated with an antibiotic cocktail for 14 days and following a two-day recovery were gavaged once per week for four weeks with or without 1×10^9 CFUs *Clostridium bifermentans* (*C. bif*) on either a low fat (LF) or high fat (HF) diet. **A)** Body weight and food intake were measured bi-weekly. **B)** Epididymal and mesenteric fat pads were weighed and expressed as a percentage of body weight. **C)** Plasma triglyceride, low density lipoprotein (LDL), non-esterified fatty acids (NEFA), and cholesterol levels were measured. **D)** Total 16S copy number was measured via qRT-PCR and expressed as per gram cecal content. Gallbladder weight (**E**), *Cckar* gene expression levels in the pancreas (**F**), and plasma cholecystokinin (CCK) and secretin (SCT) levels (**G**) were measured. **H)** Heat map displaying relative abundance of taxa (black = most abundant) in small intestine and cecal contents based on 16S rRNA amplicon sequencing data is shown. Data are shown as means +/- SEM (n=5 A-H). **A-B)** # $p \leq 0.05$ (LF+C. *bif* vs HF+C. *bif*), * $p \leq 0.05$ (LF vs HF). **B-G)** # $p \leq 0.05$ (LF vs HF), * $p \leq 0.05$ (Ctrl vs *C. bif*).

Figure S5 (related to Figure 5) Supplementation of *Lactobacillus rhamnosus* gg under LF and HF conditions. SPF mice were treated with an antibiotic cocktail for 14 days and following a two-day recovery were gavaged once per week for four weeks with or without 1×10^9 CFUs *Lactobacillus rhamnosus* gg (*L. rham*) on either a low fat (LF) or high fat (HF) diet. **A)** Body weight and food intake were measured bi-weekly. **B)** Epididymal and mesenteric fat pads were weighed and expressed as a percentage of body weight. **C)** Plasma triglyceride, low density lipoprotein (LDL), non-esterified fatty acids (NEFA), and cholesterol levels were measured. **D)** Total 16S copy number was measured via qRT-PCR and expressed as per gram cecal content. Gallbladder weight

(E), *Cckar* gene expression levels in the pancreas (F), and plasma cholecystokinin (CCK) and secretin (SCT) levels (G) were measured. H) Heat map displaying relative abundance of taxa (black = most abundant) in small intestine and cecal contents based on 16S rRNA amplicon sequencing data is shown. Data are shown as means +/- SEM (n=5 A-H). **A-B)** # $p \leq 0.05$ (LF+*L. rham* vs HF+*L. rham*), * $p \leq 0.05$ (LF vs HF). **B-G)** # $p \leq 0.05$ (LF vs HF), * $p \leq 0.05$ (Ctrl vs *L. rham*).

Figure S6 (related to Figures 1-5). Working Model. Based on our overall findings we propose that high-fat (HF) diets promote alterations in gut microbiota structure in the small intestine which leads to increased fat absorption. Microbes directly impact fatty acid (FA) uptake into absorptive enterocytes and facilitate triacylglycerol (TAG) assembly via upregulated diacylglycerol O-acyltransferase 2 (*Dgat2*) expression, mediated by microbe-derived bioactive components and/or molecules. Concurrently, microbes regulate the expression of cholecystokinin a receptor (*Cckar*) in the pancreas, allowing for detection of CCK and subsequent release of lipase for triglyceride digestion in the small intestine. Taken together, microbes regulate fat digestion and absorption via multiple mechanisms.

Table S1. Experimental Diets and Fatty Acid Composition. **Related to Figures 1-5, Figures S1-S5.**

Study Diets	Regular Chow Diet	Low Fat Diet	High Fat Diet
Fat (% kcal)	18	10.2	37.4
Saturated	2.6	1.5	24.3
C16:0 Palmitic	2.0	1.1	9.7
C18:0 Stearic	0.6	0.4	4.7
C14:0 Myristic	0	0	4.4
Other	0	0	5.5
Monounsaturated	3.5	2.4	11.9
C18:1 Oleic	3.5	2.4	10.5
Other	0	0	1.4
Polyunsaturated	9.9	6.2	1.3
C18:2 Linoleic	0	5.4	1.1
C18:3 Linolenic	0.9	0.8	0.2
Protein (% kcal)	24	13.8	15.8
Carbohydrate (% kcal)	58	76	46.8
Starch	58	66.5	11.8
Sucrose	0	14.5	23.2
Maltodextrin	0	19	11.8
Fiber (g/kg)	147	50	44.5

Table S2. Forward and reverse primer sequences used in qPCR analyses. **Related to Figure S1, Figure 3, Figure 5, Figure S4, and Figure S5.**

Gene Target	Forward	Reverse
<i>Pparγ</i>	GGA AGA CCA CTC GCA TTC CTT	GTA ATC AGC AAC CAT TGG GTC A
<i>Pparα</i>	AGA GCC CCA TCT GTC CTC TC	ACT GGT AGT CTG CAA AAC CAA A
<i>Cyp4a10</i>	TTC CCT GAT GGA CGC TCT TTA	GCA AAC CTG GAA GGG TCA AAC
<i>Cd36</i>	AGA TGA CGT GGC AAA GAA CAG	CCT TGG CTA GAT AAC GAA CTC TG
<i>Cck</i>	TAC GAA TAC CCA TCG TAG TG	GTC GTA TGT GTG GTT GTT TC
<i>Sct</i>	TCA GAG TGG ACT GAA ACA AC	TAT TGA TGC CAA GGA CAA CC
<i>Fabp1</i>	GTC AGA AAT CGT GCA TGA AGG G	GAA CTC ATT GCG GAC CAC TTT
<i>Fabp2</i>	TGC GAA CTG GAG ACC ATG AC	TCA GTC ACG GAC TTT ATG CCT
<i>Npc1l1</i>	TGT CCC CGC CTA TAC AAT GG	CCT TGG TGA TAG ACA GGC TAC TG
<i>Abcg5</i>	AGG GCC TCA CAT CAA CAG AG	GCT GAC GCT GTA GGA CAC AT
<i>Acbg8</i>	CTG TGG AAT GGG ACT GTA CTT C	TGT TGT CAC TTT CCG AGG AGA
<i>Mogat2</i>	TGG GAG CGC AGG TTA CAG A	CAG GTG GCA TAC AGG ACA GA
<i>Dgat1</i>	TCC GTC CAG GGT GGT AGT G	TGA ACA AAG AAT CTT GCA GAC GA
<i>Dgat2</i>	GCG CTA CTT CCG AGA CTA CTT	GGG CCT TAT GCC AGG AAA CT
<i>Fas</i>	GGA GGT GAT AGC CGG TAT	TGG GTA ATC CAT AGA GCC CAG
<i>Acc</i>	GAT GAA CCA TCT CCG TTG GC	GAC CCA ATT ATG AAT CGG GAG TG
<i>Srebp2</i>	TTC TGG AGA CCA TGG AGA C	GCT CTG AAA ACA AAT CAG GG
<i>Scd1</i>	TTC TTG CGA TAC ACT CTG GTG C	CGG GAT TGA ATG TTC TTG TCG T
<i>Cckar</i>	GAC AGC CTT CTT ATG AAT GGG AG	GCT GAG GTT GAT CCA GGC AG
<i>Sctr</i>	GCC CAG ATT GTG TGA TGT GC	CGG TGA GAA TAC GAT GGC TGA T
<i>Gapdh</i>	GGC AAA TTC AAC GGC ACA GT	AGA TGG TGA TGG GCT TCG C

Table S3. PCR Efficiency Results. All primer sets were tested in jejunum mucosal scrapings except for CCKa receptor (*Cckar*) and the secretin receptor (*Sctr*) which were examined using pancreatic tissue. **Related to Figure S1, Figure 3, Figure 5, and Figures S4-S5.**

Gene Target	Slope	R2 Value	PCR Efficiency
<i>Pparγ</i>	-3.68	1.00	0.87
<i>Pparα</i>	-3.95	1.00	0.79
<i>Cyp4a10</i>	-3.96	0.99	0.79
<i>Cd36</i>	-3.70	1.00	0.86
<i>Cck</i>	-3.97	1.00	0.79
<i>Secretin</i>	-4.09	0.99	0.76
<i>Fabp1</i>	-3.85	0.99	0.82
<i>Fabp2</i>	-4.17	0.99	0.74
<i>Npc111</i>	-4.08	0.98	0.76
<i>Abcg5</i>	-4.41	0.98	0.69
<i>Acbg8</i>	-4.82	0.98	0.61
<i>Mogat2</i>	-4.58	0.99	0.65
<i>Dgat1</i>	-3.79	1.00	0.84
<i>Dgat2</i>	-4.01	1.00	0.78
<i>Fas</i>	-3.71	0.99	0.86
<i>Acc</i>	-3.44	0.99	0.95
<i>Srebp2</i>	-3.87	1.00	0.81
<i>Scd1</i>	-3.69	1.00	0.87
<i>Cckar</i>	-4.01	0.98	0.78
<i>Sctr</i>	-3.49	0.97	0.94
<i>Gapdh</i>	-3.96	0.98	0.79